AJEMA GLOBAL RESEARCH NETWORK

AMERICAN Journal of Engineering, Mechanics and Architecture
Volume 3, Issue 10, 2025 ISSN (E): 2993-2637

Numerical Results of Diffusion Combustion in Turbulent Flow of Reacting Gases

Dilshodjon Ergashev
dilshod77m@gmail.com

Abstract: This paper proposes a numerical solution to the problem of symmetrical methane flow relative to the axis in infinite satellite flow and diffusion combustion. Dimensional equations in the Mises variables of the turbulent boundary layer of the interacting gases were used to model the object. The equations for the components of the gas mixture are reduced into one equation by introducing the Schwab-Zeldovich function.

To solve the problem in the Mises coordinates, a two-layer four-point nonlinear boundary separation scheme was used, and a second order along the longitudinal coordinate was given. The iterative process was used because of the nonlinearity of the storage and displacement equations of substations. Individual results of the numerical experiment are presented.

Keywords: turbulent jet, gas mixture, diffusion flame, velocity, total enthalpy, finite differences, computational experiment.

Introduction

At present, gas is the main source of thermal energy: about 70% of the energy produced and consumed in the world is consumed by gas burning, and 30% is from water, wind, solar and nuclear fuel.

At the same time, the efficiency of using natural and liquefied gas fuel is very low. In this regard, the processes of flame formation and propagation, methods of their effective management, enrichment and development of existing mathematical models are studied in depth on the basis of new achievements in the field of turbulence, injection and combustion theory.

Various methods of continuous organization of the combustion process have been developed, the theoretical bases of which are based on the theory of turbulent shock currents and theoretical states of kinetic reaction kinetics. Jet current theory is based on a simplified version of the Nef-Stokes system of equations based on the turbulent boundary layer approach.

Two methods of organizing the combustion process in the turbulent boundary layer are widely used. In the first of them, the fuel-oxygen mixture is injected separately into the combustion zone, and the method is classified by the formation of a diffusion flame.

The second method is fuel and oxygen (or oxygen mixture - air) in the form of a mixture ready for combining. Various types of these techniques have been developed to control flame characteristics (length, width, temperature, or solids). At the same time, the basic requirements are fulfilled in the design of the combustion device, for which it is desirable to carry out a theoretical study.

Theoretical work in this field is still ongoing due to the incomplete theoretical basis of chemical exothermic reactions under turbulent and turbulent flow conditions. Given the reliability and universality of the results in this area, we believe that further research is needed.In practice, the combustion process can be organized in cyclic or large volumes at low volume and high pressure by continuously introducing reactants and isolating reaction products in the same manner [1]. In the second method, chemically interacting agents can be introduced as a separate or final mixture [7]. We can study these methods based on diffusion or uniform combustion models [8].

Uniform combustion models include Bunzen burner, Arrenius law, chemical equilibrium models [9]. The mathematical model of diffusion combustion is related to the names of Burke, Schumann, B. A. Schwab and J. B. Zeldovich, where it is assumed that the combustion rate is very high and has a thin flame surface [10]. This model was developed by F.Aliyev and Z.Zhumayev for individual combustion gases and combustible gases. Although the chemical reaction rate is assumed to be infinite, diffuse combustion has a large flame length. As a result, this method is widely used in the manufacture of construction materials and the production of mercury in rotary furnaces, as well as helping to create the necessary temperature and content for heat and mass transfer in accordance with technological requirements.

A review of literature [3.7-10] shows that diffuse combustion of fuel with methane, the main component, is not sufficiently studied. Currently, methane is the main composition of natural gas produced in Uzbekistan. The main reasons for this are the "aging" of gas fields and the separation of heavy hydrocarbons from natural gas by a single or three-stage low-temperature separation method. In view of these aspects, the paper addresses methane dissipation and diffusion combustion.

A physical problem in this matter. The combustion flows through the tube, which is the radius of the gas, and spreads at the velocity of the air flow. Each gas mixture separately has its own composition and thermal properties. Fuel gas reacts with oxygen in air. The combustion rate is considered to be very high so that oxygen does not enter the fuel zone, and oxygen in the air cannot penetrate through the combustible mixture. Chemically passive gases are convective to migrate and diffuse with other components.

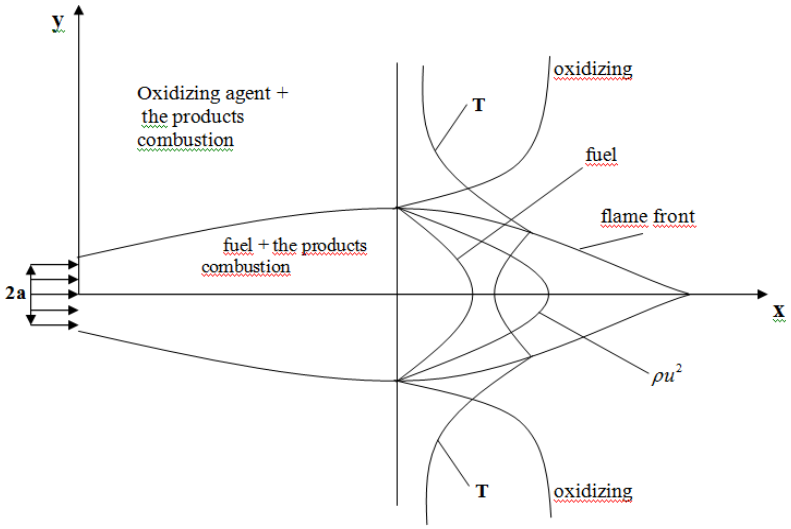

Figure 1. Schematic representation of a submerged jet with diffusion torch.

The combustion process is modeled as a stoichiometric equation of irreversible gross reaction:

Mathematical problem definition. Thermal and mass exchange processes

$$\begin{cases} \rho u\dfrac{\partial u}{\partial x}+\rho\vartheta\dfrac{\partial u}{\partial r}=\dfrac{1}{r}\dfrac{\partial}{\partial r}\left(\rho(\nu+\nu_t)r\dfrac{\partial u}{\partial r}\right), \\ \dfrac{\partial(\rho u r)}{\partial x}+\dfrac{\partial(\rho\vartheta r)}{\partial r}=0, \\ \rho u\dfrac{\partial H}{\partial x}+\rho\vartheta\dfrac{\partial H}{\partial r}=\dfrac{1}{\Pr r}\dfrac{\partial}{\partial r}\left(\rho(\nu+\nu_t)r\dfrac{\partial H}{\partial r}\right), \\ \rho u\dfrac{\partial c_2}{\partial x}+\rho\vartheta\dfrac{\partial c_2}{\partial r}=\dfrac{1}{Sc\,r}\dfrac{\partial}{\partial r}\left[\rho\left(\dfrac{1}{\mathrm{Re}}+\nu_t\right)r\dfrac{\partial c_2}{\partial r}\right]+\omega_2, \\ \rho u\dfrac{\partial c_n}{\partial x}+\rho\vartheta\dfrac{\partial c_n}{\partial r}=\dfrac{1}{Sc\,r}\dfrac{\partial}{\partial r}\left[\rho\left(\dfrac{1}{\mathrm{Re}}+\nu_t\right)r\dfrac{\partial c_n}{\partial r}\right]+\omega_n \ \ (n=1,3,4...N). \end{cases} \quad (1)$$

The system of differential equations is complemented by algebraic equations of enthalpy and gas mixture state, respectively:

$$H=c_pT+c_2h_2^*,\ c_p=\sum_{k=1}^{N}c_{pn}c_n, \qquad p=\rho\frac{R_0}{m}T=const,\quad m=\left(\sum_{n=1}^{N}m_n\ /\ c_n\right)^{-1}, \quad (2)$$

system of the equations [3,5,9]. Here u, v - Longitudinal and radial speed organizers m/s; ρ, T - gas density $\left(\kappa g\ m^{-3}\right)$ and absolute temperature (K); Pr, Sc - Prandtl and Schmidt turbulence numbers; c_k - mass concentration of components; ω_k - mass speed of combustion $\left(kg\,m^{-3}\,s^{-1}\right)$; ν_t – turbulent viscosity; H - full enthalpy;

The conditions for accessing the flow zone are as follows:

$$\begin{cases} x=0: \begin{cases} u=u_2, H=H_2, \overset{\approx}{C}=1,\ k=k_2,\ \varepsilon=\varepsilon_2, v=0 \quad 0\le y\le a \\ u=u_1, H=H_1, \overset{\approx}{C}=0,\ k=k_1,\ \varepsilon=\varepsilon_1,\ v=0 \quad a<y\le\infty \end{cases} \\ x>0: \begin{cases} \dfrac{du}{dy}=v=\dfrac{dH}{dy}=\dfrac{d\overset{''}{C}}{dy}=\dfrac{dk}{dy}=\dfrac{d\varepsilon}{dy}=0, \quad y=0 \\ u\to u_1,\ v\to 0,\ H\to H_1,\ \overset{''}{C}\to 0, k\to k_1,\ \varepsilon\to\varepsilon_1 \quad y\to y_\infty \end{cases} \end{cases} \quad (3)$$

Modeling turbulence. We used the $\boldsymbol{k-\varepsilon}$ model for turbulent exchange [1-3]:

$$\begin{cases} \rho u\dfrac{\partial k}{\partial x}+\rho\vartheta\dfrac{\partial k}{\partial r}=\dfrac{1}{\delta_\varepsilon r}\dfrac{\partial}{\partial r}\left(\rho r\nu_t\dfrac{\partial k}{\partial r}\right)+G_k-\rho\varepsilon, \\ \rho u\dfrac{\partial \varepsilon}{\partial x}+\rho\vartheta\dfrac{\partial \varepsilon}{\partial r}=\dfrac{1}{\delta_\varepsilon r}\dfrac{\partial}{\partial r}\left(\rho r\nu_t\dfrac{\partial \varepsilon}{\partial r}\right)+c_{\varepsilon1}f_1\dfrac{\varepsilon}{k}G_k-c_{\varepsilon2}\,\rho f_2\dfrac{\varepsilon^2}{k}. \end{cases} \quad \nu_t=\frac{c_\mu f_\mu k^2}{\varepsilon},\ \ R_R=\frac{\sqrt{k}\,r}{\nu},$$

$$f_1=1+\left(\frac{A_1}{f_\mu}\right)^3,\ f_2=1-e^{-R_t^2}, \quad (4)$$

$$R_t=\frac{k^2}{\nu\varepsilon},\ f_\mu=\left(1-e^{-A_\mu R_R}\right)^2\left(1+\frac{A_t}{R_t}\right),\ \mathrm{G}_k=4\rho\nu_t\left(\frac{\partial u}{\partial r}\right)^2,\ c_{\varepsilon2}=1.92,\ c_\mu=0.09,\ \delta_k=1\ ,\ c_{\varepsilon1}=1.44,$$

$$\delta_\varepsilon=1.3,\ A_1=0.05,\ A_\mu=0.0165$$

A method of bringing component retention equations to a single equation. The task of spreading and burning methane gas in the satellite air flow is considered. We believe that methane has equal concentrations in combustible gas. The stoichiometric equation of the process can be written as

$$\nu_2 A + \nu_1 O_2 \rightarrow \nu_3 CO_2 + \nu_4 H_2 O + h_2^*,$$

where stoichiometric coefficients $\nu_1 = 2.0$ $\nu_2 = 1$, $\nu_3 = 1.0$, $\nu_4 = 2.0$, Refer to oxygen, combustible, carbon monoxide and water vapor; $h_2^* = 55644$. In addition, the presence of molecular nitrogen is taken into account N_2, Which is considered a chemically passive component. Accordingly, in this case, the number of component retention equations is $N = 5$, which are abbreviated as $L(c_k) = \omega_k$ $(k = 1..5)$. Where $L(c_k) = \rho u \frac{\partial c_k}{\partial x} + \rho v \frac{\partial c_k}{\partial y} - \frac{1}{Sc\, y} \frac{\partial}{\partial y}\left(\rho \varepsilon y \frac{\partial c_k}{\partial y} \right)$ – Linear and uniform with respect to its argument - mass concentration k - component c_k operator, and ω_k – Mass rate of formation (disappearance) k -ro the variety of molecules at a given point of the flame front for a single period of time. For chemical reaction rates, the following relationships occur where considered

$$\begin{aligned} &\omega_3 \nu_k m_k + \omega_k \nu_3 m_3 = 0 \quad \text{при} \quad k = 1,2; \\ &\omega_3 \nu_k m_k - \omega_k \nu_3 m_3 = 0 \quad \text{при} \quad k = 4; \end{aligned} \qquad (5)$$

$$\omega_1,\ \omega_2 \le 0,\ \omega_3,\ \omega_4 \ge 0.$$

The dependencies given indicate the path by which the chemical reaction rates can be eliminated in the component conservation equations $L(c_k) = \omega_k$.

If you enter Schwab-Zeldovich functions according to,

$$\tilde{C}_k = \begin{cases} c_3 \nu_k m_k + c_k \nu_3 m_3 = 0 \quad \text{при} \quad k = 1,2; \\ c_3 \nu_k m_k - c_k \nu_3 m_3 = 0 \quad \text{при} \quad k = 4, \end{cases} \qquad (6)$$

then the component conservation equations for $k = 1,2$ and 4 take on the stock-free form $L(\tilde{C}_k) = 0$.

The equation for inert gas concentration, since $\omega_5 = 0$, is also similar to $L(c_5) = 0$. I.e. We have four differential equations for five concentrations of components. The missing equation is replaced by the assumptions of the diffusion combustion model.

We will draw up boundary conditions for the entered functions:

$$\begin{aligned} &\left(\tilde{C}_1\right)_1 = (c_3)_1 \nu_1 m_1 + (c_1)_1 \nu_3 m_3, \quad \left(\tilde{C}_1\right)_2 = (c_3)_2 \nu_1 m_1, \\ &\left(\tilde{C}_2\right)_1 = (c_3)_1 \nu_2 m_2, \quad \left(\tilde{C}_2\right)_2 = (c_3)_2 \nu_2 m_2 + (c_2)_2 \nu_3 m_3, \\ &\left(\tilde{C}_4\right)_1 = (c_3)_1 \nu_4 m_4 - (c_4)_1 \nu_3 m_3, \quad \left(\tilde{C}_4\right)_2 = (c_3)_2 \nu_4 m_4 - (c_4)_2 \nu_3 m_3. \end{aligned} \qquad (7)$$

Now we will enter relatively redundant functions relative to $\tilde{C}_k$

$$\tilde{\tilde{C}}_k = \frac{\tilde{C}_k - \left(\tilde{C}_k\right)_1}{\left(\tilde{C}_k\right)_2 - \left(\tilde{C}_k\right)_1} = \frac{c_5 - (c_5)_1}{(c_5)_2 - (c_5)_1}. \qquad (8)$$

Analysis shows that equations $L(\tilde{\tilde{C}}_k)=0$ are mutually equivalent because they have the same coefficients and boundary conditions. This will allow four equations $L(\tilde{\tilde{C}}_k)=0$ to go to a single equation $L\left(\tilde{\tilde{C}}\right)=0$.

In particular, at the fuel zone inlet this function has a value of 1, at the oxidizer zone inlet and at the jet boundary it has a value of 0. There is symmetry on the jet axis for a given function.

With the known value of this function, the concentration of the inert gas is determined simply:

$$C_5=(C_5)_1+\left[(C_5)_2-(C_5)_1\right]\tilde{\tilde{C}}.\ \tilde{C}_k=\left(\tilde{C}_k\right)_1+\left[\left(\tilde{C}_k\right)_2-\left(\tilde{C}_k\right)_1\right]\tilde{\tilde{C}}.$$

Substitution of values $\tilde{C}_k$, $\left(\tilde{C}_k\right)_2$, $\left(\tilde{C}_k\right)_1$ in these constraints lead to a system of linear equations

$$\begin{cases} c_3\nu_1 m_1+c_1\nu_3 m_3=(c_3)_1\nu_1 m_1+(c_1)_1\nu_3 m_3+ \\ \quad +\left[(c_3)_2\nu_1 m_1-(c_3)_1\nu_1 m_1-(c_1)_1\nu_3 m_3\right]\tilde{\tilde{C}}, \\ c_3\nu_2 m_2+c_2\nu_3 m_3=(c_3)_1\nu_2 m_2+ \\ \quad +\left[(c_3)_2\nu_2 m_2+(c_2)_2\nu_3 m_3-(c_3)_1\nu_2 m_2\right]\tilde{\tilde{C}}, \\ c_3\nu_4 m_4-c_4\nu_3 m_3=(c_3)_1\nu_4 m_4-(c_4)_1\nu_3 m_3+ \\ \quad +\left[(c_3)_2\nu_4 m_4-(c_4)_2\nu_3 m_3-(c_3)_1\nu_4 m_4+(c_4)_1\nu_3 m_3\right]\tilde{\tilde{C}}. \end{cases} \quad (9)$$

Let's simplify a system:

$$\begin{cases} c_3+c_1\dfrac{\nu_3 m_3}{\nu_1 m_1}=(c_3)_1+(c_1)_1\dfrac{\nu_3 m_3}{\nu_1 m_1}+\left[(c_3)_2-(c_3)_1-(c_1)_1\dfrac{\nu_3 m_3}{\nu_1 m_1}\right]\tilde{\tilde{C}}, \\ c_3+c_2\dfrac{\nu_3 m_3}{\nu_2 m_2}=(c_3)_1+\left[(c_3)_2-(c_3)_1+(c_2)_2\dfrac{\nu_3 m_3}{\nu_2 m_2}\right]\tilde{\tilde{C}}, \\ c_3-c_4\dfrac{\nu_3 m_3}{\nu_4 m_4}=(c_3)_1-(c_4)_1\dfrac{\nu_3 m_3}{\nu_4 m_4}+ \\ +\left[(c_3)_2-(c_3)_1-\left((c_4)_2-(c_4)_1\right)\dfrac{\nu_3 m_3}{\nu_4 m_4}\right]\tilde{\tilde{C}}. \end{cases} \quad (10)$$

On the flame phonta, the reactant concentrations are zero. In this case, from the first two equations of this system, the value of the relatively-redundant function corresponding to the flame front is determined:

$\tilde{\tilde{C}}^*=\left[1+\dfrac{(c_2)_2}{(c_1)_1}\dfrac{\nu_1 m_1}{\nu_2 m_2}\right]^{-1}$ at $\tilde{\tilde{C}}^*<\tilde{\tilde{C}}\le 1$, there is no oxidant in the fuel zone – $c_1=0$. The solution of the system is

$$c_2=\left[(c_2)_2+(c_1)_1\frac{\nu_2 m_2}{\nu_1 m_1}\right]\tilde{\tilde{C}}-(c_1)_1\frac{\nu_2 m_2}{\nu_1 m_1},\ c_3=(c_3)_1+(c_1)_1\frac{\nu_3 m_3}{\nu_1 m_1}+\left[(c_3)_2-(c_3)_1-(c_1)_1\frac{\nu_3 m_3}{\nu_1 m_1}\right]\tilde{\tilde{C}},$$

$$c_4=(c_4)_1+(c_1)_1\frac{\nu_4 m_4}{\nu_1 m_1}+\left[(c_4)_2-(c_4)_1-(c_1)_1\frac{\nu_4 m_4}{\nu_1 m_1}\right]\tilde{\tilde{C}}. \quad (11)$$

Conditions $0 \le \tilde{\tilde{C}} < \tilde{\tilde{C}}^*$ oxidant zone where there is no fuel is determined $c_2 = 0$. The concentrations of the remaining components are determined by the formulae:

$$c_1 = (c_1)_1 - \left[(c_1)_1 + (c_2)_2 \frac{\nu_1 m_1}{\nu_2 m_2} \right] \tilde{\tilde{C}},$$

$$c_3 = (c_3)_1 + \left[(c_3)_2 - (c_3)_1 + (c_2)_2 \frac{\nu_3 m_3}{\nu_2 m_2} \right] \tilde{\tilde{C}}, \quad (12)$$

$$c_4 = (c_4)_1 + \left[(c_4)_2 - (c_4)_1 + (c_2)_2 \frac{\nu_4 m_4}{\nu_2 m_2} \right] \tilde{\tilde{C}}.$$

Verification of the resulting formulas for concentrations can be performed by calculating the sum of the concentrations. When accounting dependences

$$(c_2)_2 + (c_3)_2 + (c_4)_2 + (c_5)_2 = 1,$$

$$(c_1)_1 + (c_3)_1 + (c_4)_1 + (c_5)_1 = 1 \quad (13)$$

and mass balance according to the stoichiometric reaction equation

$$\nu_1 m_1 + \nu_2 m_2 = \nu_3 m_3 + \nu_4 m_4 \quad (14)$$

summation of concentrations in each zone is one, although mass concentrations of components depend on the variable $\tilde{\tilde{C}}$.

Thus, depending on the value of the relative-redundant function $\tilde{\tilde{C}}$ positions of flame front and concentration of components are unambiguously determined. The boundary conditions for this function are, as noted above,

$$\tilde{\tilde{C}}(0, y) = \begin{cases} 1 & 0 \le y \le a, \\ 0 & y > a, \end{cases} \quad \frac{\partial \tilde{\tilde{C}}(x,0)}{\partial x} = 0, \quad \tilde{\tilde{C}}(x, y_\infty) \to 0. \quad (15)$$

Chemical reaction with final rate modeling. The combustion process is modeled in the form of a stoichiometric equation of the irreversible gross reaction**:**

$CH_4 + 2O_2 = CO_2 + 2H_2O + h_2^*$, is here h_2^* – the amount of heat released by an exothermic reaction. The reaction rate is modeled on the Arrenius law [3]. $\omega_2 = A_{r1} c_1 c_2 \rho^2 \exp\left(-\frac{A_{r2}}{T} \right)$. Here entered designations

$$A_{r1} = -5,028 \cdot 10^{11} \frac{a \rho_2}{m_1 u_2}, \quad A_{r2} = \frac{200010.0}{8,31441} (K)$$

Tangential disturbance in the common boundary of intermediate flows and presence of high-temperature flame front in the area of heat-mass transfer indicate turbulence of flow in this area. Due to the presence of the main flow direction, turbulent boundary layer equations can be used in the movement of gases.

Introduction of dimensionless and Mises variables. To solve the problem, you went to dimensionless coordinates using characteristic values a, u_2, H_2, ρ_2:

$$\bar{x} = \frac{x}{a}, \quad \bar{r} = \frac{r}{a}, \quad \bar{u} = \frac{u}{u_2}, \quad \bar{v} = \frac{v}{u_2}, \quad \bar{\varepsilon} = \frac{\varepsilon}{a u_2},$$

$$\bar{H}=\frac{H}{H_2},\ \bar{\rho}=\frac{\rho}{\rho_2},\ \ \bar{T}=\frac{T}{T_2},\ \ \bar{p}=\frac{p}{\rho_2 u_2^2},\ \ \bar{h}_2^*=\frac{h_2^*}{H_2}. \quad (16)$$

For example, the fuel storage and transfer equation takes the form:

$$\rho_2\bar{\rho}u_2\bar{u}\frac{\partial c_2}{a\partial\bar{x}}+\rho_2\bar{\rho}u_2\bar{v}\frac{\partial c_2}{a\partial\bar{r}}=\frac{1}{\mathrm{Sc}a\bar{r}}\frac{\partial}{a\partial\bar{r}}\left[\rho_2\bar{\rho}au_2\left(\frac{1}{\mathrm{Re}}+\bar{\nu}_t\right)a\bar{r}\frac{\partial c_2}{a\partial\bar{r}}\right]-$$

$$-7\cdot10^8\frac{c_1c_2\rho_2^2\bar{\rho}^2}{m_1}\exp\left(-\frac{190300}{8{,}31441T}\right),$$

where the dimension ω_2 was transferred to SI and also taken into account $\rho_1=c_1\rho$ и $\rho_2=c_2\rho$.

Now multiply both sides of the equation by $\frac{a}{\rho_2u_2}$, also we will receive

$$\bar{\rho}\bar{u}\frac{\partial c_2}{\partial\bar{x}}+\bar{\rho}\bar{v}\frac{\partial c_2}{\partial\bar{r}}=\frac{1}{Sc\,\bar{r}}\frac{\partial}{\partial\bar{r}}\left[\bar{\rho}\left(\frac{1}{\mathrm{Re}}+\bar{\nu}_t\right)\bar{r}\frac{\partial c_2}{\partial\bar{r}}\right]+A_{r1}c_1c_2\bar{\rho}^2\exp\left(-\frac{A_{r2}}{T}\right).$$

$$\begin{cases}
\bar{\rho}\bar{u}\dfrac{\partial\bar{u}}{\partial\bar{x}}+\bar{\rho}\bar{\vartheta}\dfrac{\partial\bar{u}}{\partial\bar{r}}=\dfrac{\partial}{\bar{r}\partial r}\left[\bar{\rho}\left(\dfrac{1}{\mathrm{Re}}+\bar{\nu}_t\right)\bar{r}\dfrac{\partial\bar{u}}{\partial\bar{r}}\right],\\
\dfrac{\partial\left(\bar{\rho}\bar{u}\bar{r}\right)}{\partial\bar{x}}+\dfrac{\partial\left(\bar{\rho}\bar{\vartheta}\bar{r}\right)}{\partial\bar{r}}=0,\\
\bar{\rho}\bar{u}\dfrac{\partial\bar{\bar{H}}}{\partial\bar{x}}+\bar{\rho}\bar{\vartheta}\dfrac{\partial\bar{\bar{H}}}{\partial\bar{r}}=\dfrac{1}{\mathrm{Pr}\,\bar{r}}\dfrac{\partial}{\partial\bar{r}}\left[\bar{\rho}\left(\dfrac{1}{\mathrm{Re}}+\bar{\nu}_t\right)\bar{r}\dfrac{\partial\bar{\bar{H}}}{\partial\bar{r}}\right],\\
\bar{\rho}\bar{u}\dfrac{\partial\bar{c}_2}{\partial\bar{x}}+\bar{\rho}\bar{\vartheta}\dfrac{\partial\bar{c}_2}{\partial\bar{r}}=\dfrac{1}{Sc\bar{r}}\dfrac{\partial}{\partial\bar{r}}\left[\bar{\rho}\left(\dfrac{1}{\mathrm{Re}}+\bar{\nu}_t\right)\bar{r}\dfrac{\partial\bar{c}_2}{\partial\bar{r}}\right]+A_{r1}c_1c_2\bar{\rho}^2\exp(-A_{r2}/T),\\
\bar{\rho}\bar{u}\dfrac{\partial\bar{\bar{C}}}{\partial\bar{x}}+\bar{\rho}\bar{\vartheta}\dfrac{\partial\bar{\bar{C}}}{\partial\bar{r}}=\dfrac{1}{Sc\bar{r}}\dfrac{\partial}{\partial\bar{r}}\left[\bar{\rho}\left(\dfrac{1}{\mathrm{Re}}+\bar{\nu}_t\right)\bar{r}\dfrac{\partial\bar{\bar{C}}}{\partial\bar{r}}\right],\\
\bar{\rho}\bar{u}\dfrac{\partial\bar{k}}{\partial\bar{x}}+\bar{\rho}\bar{\vartheta}\dfrac{\partial\bar{k}}{\partial\bar{r}}=\dfrac{1}{\delta_k\bar{r}}\dfrac{\partial}{\partial\bar{r}}\left(\bar{\rho}\bar{\nu}_t\bar{r}\dfrac{\partial\bar{k}}{\partial r}\right)+4\bar{\rho}\bar{\nu}_t\left(\dfrac{\partial\bar{u}}{\partial\bar{r}}\right)^2-\bar{\rho}\bar{\varepsilon},\\
\bar{\rho}\bar{u}\dfrac{\partial\bar{\varepsilon}}{\partial\bar{x}}+\bar{\rho}\bar{\vartheta}\dfrac{\partial\bar{\varepsilon}}{\partial\bar{r}}=\dfrac{1}{\delta_\varepsilon\bar{r}}\dfrac{\partial}{\partial\bar{r}}\left(\bar{\rho}\bar{\nu}_t\bar{r}\dfrac{\partial\bar{\varepsilon}}{\partial\bar{r}}\right)+4c_1\left[1+\dfrac{A_1}{f_\mu}\right]^3\bar{\rho}\bar{\nu}_t\dfrac{\bar{\varepsilon}}{\bar{\bar{k}}}\left(\dfrac{\partial\bar{u}}{\partial\bar{r}}\right)^2-\\
-c_2\left(1-e^{-\frac{\bar{k}^4}{\mathrm{Re}^2\bar{\varepsilon}^2}}\right)\bar{\rho}\dfrac{\bar{\varepsilon}^2}{\bar{k}}.
\end{cases} \quad (17)$$

Here entered designation $f_\mu=\left(1-e^{-A_\mu\mathrm{Re}\sqrt{\bar{k}}r}\right)^2\left(1+A_t\frac{\bar{\varepsilon}}{\mathrm{Re}\,\bar{k}^2}\right)$.

$$T=\frac{H_1+\left(H_2-H_1\right)\bar{\bar{H}}-c_2h_2^*}{c_p},\ \ \bar{\nu}_t=c_\mu f_\mu\frac{\bar{k}^2}{\bar{\varepsilon}}. \quad (18)$$

Since straight-flow free expanded jets are considered, on the basis of data known from the theory and practice in the field of flow, the value of static pressure is taken to be constant: $p=const$ (according to Bai Shi-I for jet currents without burning, the change in static pressure is not more than 0.5% of dynamic pressure, and for jets with burning this fact is confirmed by experimental and theoretical Spaulding data). As a result, the equation of the state of the gas mixture becomes

$$\bar{\rho}=\frac{m}{(m)_2\bar{T}}. \quad (19)$$

The second feature of the problem is that the flow propagates along the x axis from left to right and there are no boundary conditions in the right part of the flow area, as it does not affect the propagation processes. Accordingly, the process is suitably described by parabolic equations. Therefore, we use the Mises coordinates and introduce the current function according to the relations:

$$\rho u r = \psi \frac{\partial \psi}{\partial r}, \quad \rho v r = -\psi \frac{\partial \psi}{\partial x}. \quad (20)$$

The second equation of the system is satisfied unambiguously. We find the value of transverse coordinate required for calculation by formula $\frac{r^2}{2} = \int_0^{\psi} \frac{\psi d\psi}{\rho u}$. In other equations of the system, transition from coordinates (x, y) to coordinates (ξ, ψ) is performed by formulas:

$$\frac{\partial}{\partial x} = \frac{\partial}{\partial \xi} + \frac{\partial \psi}{\partial x}\frac{\partial}{\partial \psi} = \frac{\partial}{\partial \xi} - \frac{r}{\psi}\rho v \frac{\partial}{\partial \psi}, \quad (21)$$
$$\frac{\partial}{\partial r} = \frac{\partial \psi}{\partial r}\frac{\partial}{\partial \psi} = \frac{r}{\psi}\rho u \frac{\partial}{\partial \psi}.$$

This converts the right sides of the equations as

$$\rho u \frac{\partial}{\partial x} + \rho v \frac{\partial}{\partial r} =$$
$$= \rho u \left[\frac{\partial}{\partial \xi} - \frac{r}{\psi}\rho v \frac{\partial}{\partial \psi} \right] + \rho v \frac{r}{\psi}\rho u \frac{\partial}{\partial \psi} = \rho u \frac{\partial}{\partial \xi}.$$

The left parts of the equations are converted as

$$\frac{1}{r}\frac{\partial}{\partial r}\left(\rho \varepsilon r \frac{\partial}{\partial r} \right) = \frac{1}{r}\frac{r}{\psi}\rho u \frac{\partial}{\partial \psi}\left(\rho \varepsilon r \frac{r}{\psi}\rho u \frac{\partial}{\partial \psi} \right) =$$
$$= \frac{1}{\psi}\rho u \frac{\partial}{\partial \psi}\left(\frac{\rho^2 \varepsilon r^2 u}{\psi}\frac{\partial}{\partial \psi} \right).$$

$$\begin{cases} \dfrac{\partial u}{\partial \xi} = \dfrac{1}{\psi}\dfrac{\partial u}{\partial \psi}\left[\dfrac{\rho^2 u\, r^2 (\nu + \nu_t)}{\psi}\dfrac{\partial u}{\partial \psi} \right], \\ \dfrac{\partial H}{\partial \xi} = \dfrac{1}{\mathrm{Pr}\psi}\dfrac{\partial}{\partial \psi}\left[\dfrac{\rho^2 u\, r^2 (\nu + \nu_t)}{\psi}\dfrac{\partial u}{\partial \psi} \right], \\ \dfrac{\partial c_2}{\partial \xi} = \dfrac{1}{\mathrm{Sc}\psi}\dfrac{\partial}{\partial \psi}\left[\dfrac{\rho^2 u r^2 (\nu + \nu_t)}{\psi}\dfrac{\partial c_2}{\partial \psi} \right] + A_{r1}\dfrac{c_1 c_2 \rho^2}{u}\exp(-A_{r2}/T), \\ \dfrac{\partial \overline{\overline{C}}}{\partial \xi} = \dfrac{1}{\mathrm{Sc}\psi}\dfrac{\partial}{\partial \psi}\left[\dfrac{\rho^2 u r^2 (\nu + \nu_t)}{\psi}\dfrac{\partial \overline{\overline{C}}}{\partial \psi} \right], \\ \dfrac{\partial k}{\partial \xi} = \dfrac{1}{\psi}\dfrac{\partial}{\partial \psi}\left(\dfrac{r^2 u \rho^2}{\psi}\dfrac{\nu_t}{\delta_k}\dfrac{\partial k}{\partial \psi} \right) + 4\dfrac{\rho^2 r^2 u}{\psi^2}\nu_t \left(\dfrac{\partial u}{\partial \psi} \right)^2 - \dfrac{\varepsilon}{u}, \\ \dfrac{\partial \varepsilon}{\partial \xi} = \dfrac{1}{\delta_\varepsilon \psi}\dfrac{\partial}{\partial \psi}\left(\dfrac{\rho^2 u r^2}{\psi}\nu_t \dfrac{\partial \varepsilon}{\partial \psi} \right) + \\ + c_1 \left[1 + \left(A_1 / f_\mu \right)^3 \right]\dfrac{\varepsilon}{k} 4\dfrac{\rho^2 u r^2}{\psi^2}\nu_t \left(\dfrac{\partial u}{\partial \psi} \right)^2 - c_2 \left(1 - e^{-\frac{k^4}{\mathrm{Re}^2 \varepsilon^2}} \right)\dfrac{\varepsilon^2}{ku}, \end{cases} \quad (22)$$

SOLUTION METHOD

Numerical way to solve the problem. Using basic radius a, flow rate u_2, density ρ_2, and enthalpy H_2, measurements were made in the system and conditions of equations, and Mises coordinates were entered (ξ,ψ). The mass displacement and retention equations for the components were reduced into one equation by introducing Schwab-Zeldovich functions and relative peak concentration $\tilde{\tilde{C}}$ [3,5]. As a result, the basic equations

$$\begin{cases} \dfrac{\partial u}{\partial \xi}=\dfrac{1}{\psi}\dfrac{\partial u}{\partial \psi}\left[\dfrac{\rho^2 u\, r^2(\nu+\nu_t)}{\psi}\dfrac{\partial u}{\partial \psi}\right], \\ \dfrac{\partial H}{\partial \xi}=\dfrac{1}{\mathrm{Pr}\psi}\dfrac{\partial}{\partial \psi}\left[\dfrac{\rho^2 u\, r^2(\nu+\nu_t)}{\psi}\dfrac{\partial u}{\partial \psi}\right], \\ \dfrac{\partial c_2}{\partial \xi}=\dfrac{1}{\mathrm{Sc}\psi}\dfrac{\partial}{\partial \psi}\left[\dfrac{\rho^2 u r^2(\nu+\nu_t)}{\psi}\dfrac{\partial c_2}{\partial \psi}\right]+A_{r1}\dfrac{\mathrm{c_1 c_2}\,\bar{\rho}^2}{u}\exp(-\mathrm{A}_{r2}/\mathrm{T}), \\ \dfrac{\partial \tilde{\tilde{C}}}{\partial \xi}=\dfrac{1}{\mathrm{Sc}\psi}\dfrac{\partial}{\partial \psi}\left[\dfrac{\rho^2 u r^2(\nu+\nu_t)}{\psi}\dfrac{\partial \tilde{\tilde{C}}}{\partial \psi}\right], \\ \dfrac{\partial k}{\partial \xi}=\dfrac{1}{\psi}\dfrac{\partial}{\partial \psi}\left(\dfrac{r^2 u\rho^2}{\psi}\dfrac{\nu_t}{\delta_k}\dfrac{\partial k}{\partial \psi}\right)+4\dfrac{\rho^2 r^2 u}{\psi^2}\bar{\nu}_t\left(\dfrac{\partial u}{\partial \psi}\right)^2-\dfrac{\varepsilon}{u}, \\ \dfrac{\partial \varepsilon}{\partial \xi}=\dfrac{1}{\psi}\dfrac{\partial}{\partial \psi}\left(\dfrac{\rho^2 r^2 u}{\psi}\dfrac{\nu_t}{\delta_\varepsilon}\dfrac{\partial \varepsilon}{\partial \psi}\right)+4\dfrac{c_1\rho^2 r^2 u}{\psi^2}\bar{\nu}_t\dfrac{\varepsilon}{k}\times \\ \times\left[1+A_1\left(1-\mathrm{e}^{A_\mu \mathrm{Re}\sqrt{\bar{k}}r}\right)^{-2}\left(1+\dfrac{A_t\bar{\varepsilon}}{\mathrm{Re}\bar{k}^2}\right)^{-1}\right]^3\left(\dfrac{\partial u}{\partial \psi}\right)^2-c_2\left(1-e^{\frac{-\mathrm{Re}^2\varepsilon^2}{k^4}}\right)\dfrac{\varepsilon^2}{ku}, \end{cases} \quad (23)$$

$$T=\frac{H_1+(H_2-H_1)\bar{\bar{H}}-c_2h_2^*}{c_p},$$

$$\bar{\rho}=\frac{mT_2}{(\mathrm{m})_2 T},\ \bar{\nu}_t=c_\mu f_\mu\frac{\bar{k}^2}{\bar{\varepsilon}}.$$

and corresponding boundary conditions were formed.

$0\le\bar{\psi}<1:\bar{u}=1,\bar{T}=1,\bar{\bar{C}}=1,\ c_n=(c_n)_2,k=k_2,\varepsilon=\varepsilon_2.1\le\bar{\psi}<\bar{\psi}_\infty:$

$\bar{u}=\bar{u}_1,\bar{T}=\bar{T}_1,\bar{\bar{C}}=0,c_n=(c_n)_1,k=k_1,\varepsilon=\varepsilon_1.$

$$\xi>0\ ,\psi=0:\ \frac{\partial\bar{u}}{\partial\bar{\psi}}=0,\frac{\partial\bar{T}}{\partial\bar{\psi}}=0,\frac{\partial\bar{\bar{C}}}{\partial\psi}=0,\frac{\partial c_2}{\partial\psi}=0,\ \frac{\partial\bar{k}}{\partial\bar{\psi}}=0,\frac{\partial\varepsilon}{\partial\psi}=0. \quad (24)$$

$\psi\to\psi_\infty:\bar{u}=\bar{u}_1,\ \bar{T}=\bar{T}_1,c_2=(c_2)_1,\bar{\bar{C}}=0,\ k=k_1,\ \varepsilon=\varepsilon_1.$

The constant approximation scheme was used to solve nonlinear equations in Mizes coordinates. [9-11].

$$\frac{\partial U}{\partial\bar{\xi}}=\frac{1}{\delta_U}\frac{\partial}{\bar{\psi}\partial\bar{\psi}}\left(K\lambda h_\psi\frac{\partial U}{\partial\bar{\psi}}\right)+f_U. \quad (25)$$

In the first group, where $\lambda=\dfrac{1}{\mathrm{Re}}+\nu_t$, enter

$$U = u:\ \delta_U = 1,\ f_U = 0;$$
$$U = \bar{\bar{H}}:\ \delta_H = \mathrm{Pr},\ f_H = 0;$$
$$U = \bar{\bar{C}}:\ \delta_C = Sc,\ f_C = 0; \qquad (26)$$
$$U = c_2:\ \delta_{c2} = Sc,\ f_{c2} = A_{r1}\frac{c_1 c_2 \bar{\rho}}{\bar{u}}\exp(-A_{r2}/T).$$

To old group where accepted $\lambda = \nu_t$, there are two remaining equations:

$$U = k:\ \delta_U = \delta_k,\ f_k = 4\frac{Kh_\psi}{\bar{\psi}}\lambda\left(\frac{\partial\bar{u}}{\partial\bar{\psi}}\right)^2 - \frac{\bar{\varepsilon}}{\bar{u}} = \bar{\mathrm{E}} - \frac{\bar{\varepsilon}}{\bar{u}},$$
$$U = \varepsilon:\ \delta_U = \delta_\varepsilon,\ f_\varepsilon = \bar{E}\frac{\bar{\varepsilon}}{\bar{k}}\left[1 + \left(\frac{A_1}{f_\mu}\right)^3\right] - c_2\left(1 - e^{\frac{-k^4}{\varepsilon^2\,\mathrm{Re}^2}}\right)\frac{\bar{\varepsilon}^2}{\bar{k}}. \qquad (27)$$

We come to the approximation of equations. For the first group we have:

$$\lambda_j = \frac{1}{\mathrm{Re}} + (\bar{\nu}_t)_{i,j};$$
$$\frac{U^s_{i,j} - U_{i-1,j}}{h_\xi} = \frac{1}{2Sc_u j h^2_\psi}\times\Big[\left(K_{i,j+1}\lambda_{j+1} + K_{i,j}\lambda_j\right)\left(U^s_{i,j+1} - U^s_{i,j}\right) -$$
$$-\left(K_{i,j}\lambda_j + K_{i,j-1}\lambda_{j-1}\right)\left(U^s_{i,j} - U^s_{i,j-1}\right)\Big] + \left(f_u\right)^{s-1}_{i,j},$$

Multiply both sides of the equation by $2Sc_u h_\xi j$ also we will enter designation $\sigma = h_\xi / h^2_\psi$. Then we will receive

$$\sigma\left(K_{i,j+1}\lambda_{j+1} + K_{i,j}\lambda_j\right)U^s_{i,j+1} -$$
$$-\Big[2Sc_u j + \sigma\left(K_{i,j+1}\lambda_{j+1} + K_{i,j}\lambda_j\right) + \sigma\left(K_{i,j}\lambda_j + K_{i,j-1}\lambda_{j-1}\right)\Big]U^s_{i,j} +$$
$$+\sigma\left(K_{i,j}\lambda_j + K_{i,j-1}\lambda_{j-1}\right)U^s_{i,j-1} = -2Sc_u j\left(U_{i-1,j} + h_\xi\left(f_u\right)^{s-1}_{i,j}\right).$$

Let's designate

$$a^{(\mathrm{U})}_j = \sigma\left(K_{i,j+1}\lambda_{j+1} + K_{i,j}\lambda_j\right),\ c^{(\mathrm{U})}_j = \sigma\left(K_{i,j}\lambda_j + K_{i,j-1}\lambda_{j-1}\right),$$
$$b^{(\mathrm{U})}_j = 2Sc_U j + a^{(\mathrm{U})}_j + c^{(\mathrm{U})}_j,\ d^{(\mathrm{U})}_j = -2Sc_U j\left(U_{i-1,j} + h_\xi\left(f_U\right)^{s-1}_{i,j}\right).$$

Then the finite difference equation takes the form:

$$a^{(\mathrm{U})}_j U^s_{i,j+1} - b^{(\mathrm{U})}_j U^s_{i,j} + c^{(\mathrm{U})}_j U^s_{i,j-1} = d^{(\mathrm{U})}_j. \qquad (28)$$

If we believe that

$$U^s_{i,j-1} = \alpha^{(\mathrm{U})}_{j-1} U^s_{i,j} + \beta^{(\mathrm{U})}_{j-1},$$

Then we get values of fit coefficients for internal nodes:

$$\alpha^{(\mathrm{U})}_j = \frac{a^{(\mathrm{U})}_j}{b^{(\mathrm{U})}_j - \alpha^{(\mathrm{U})}_{j-1}c^{(\mathrm{U})}_j},\ \beta^{(\mathrm{U})}_j = \frac{-d^{(\mathrm{U})}_j + c^{(\mathrm{U})}_j\beta^{(\mathrm{U})}_{j-1}}{b^{(\mathrm{U})}_j - \alpha^{(\mathrm{U})}_{j-1}c^{(\mathrm{U})}_j} \qquad (29)$$

The first $S_{\min}$ approach is performed without check of approach condition and replacement

$$\begin{aligned} \overset{\approx}{u}_{i,j}^{s-1} &= \overset{\approx}{u}_{i,j}^{s}, \quad \overset{\approx}{H}_{i,j}^{s-1} = \overset{\approx}{H}_{i,j}^{s}, \\ \rho_{i,j}^{s-1} &= \rho_{i,j}^{s}, \quad \overset{\approx}{C}_{i,j}^{s-1} = \overset{\approx}{C}_{i,j}^{s} \end{aligned} \quad . (30)$$

Later $S_{\min}$ - the convergence condition is checked $\max_{j\in[0;\,N_j]}\left|\overset{\approx}{H}_{i,j}^{s-1}-\overset{\approx}{H}_{i,j}^{s}\right|<\varepsilon_t$.

If convergence conditions are reached, the system moves to the next layer at. Otherwise, the s-th approach is accepted

$$\begin{aligned} \overset{\approx}{u}_{i,j}^{s-1} &= \overset{\approx}{u}_{i,j}^{s}, \quad \overset{\approx}{H}_{i,j}^{s-1} = \overset{\approx}{H}_{i,j}^{s}, \\ \rho_{i,j}^{s-1} &= \rho_{i,j}^{s}, \quad \overset{\approx}{C}_{i,j}^{s-1} = \overset{\approx}{C}_{i,j}^{s} \end{aligned}$$

and proceeds to the next approximation.

If all requirements for accuracy of newly found parameter values are satisfied, if necessary, values of integrals of excess pulse, enthalpy, as well as unburned part of fuel in this section are calculated.

The upper limit of the dimensionless coordinates of the flow curve was taken as 20 and new discrete steps for longitudinal and radial coordinates were introduced. The calculation of the longitudinal coordinate continued until the conservative function value on the axis dropped to 0.05.

After these steps, the results were saved in three files. The first file contained the axis speed, enthalpy, turbulence factor for cross section, radial flame coordinates determined by linear interpolation, boundary layer speed limit $b(x)$, and observational data.

The second file contains information on changes in radial coordinate functions of velocity, enthalpy, temperature, concentration and turbulence at certain sites. In this case, a special algorithm was used to switch from the regular step of the flow line function to the dimensionless radial coordinate, using the linear interpolation formula in h_y algorithms for graphical drawing.

In the third file, the data required to construct the isothermal curves in the temperature calculation area was stored in unobstructed coordinates. Due to limitations of some of the measurements considered, particularly the computing domain, the graphics capabilities of Pascal ABS computer graphics were not available. Because of this, the resulting data was rendered using Excel software.

RESULTS

In the article, we limit ourselves to the discussion of the effect of the temperature of the separate gases on isotherms and concentrations.

The combustible reaction includes methane gas and nitrogen. $(c_1)_1 = 0.232,\ (c_5)_1 = 0.768, (c_2)_2 = 1$. The velocity of the main stream - 61 m/s, velocity of satellite current – 18.3 m/s. $T_1 = 1000\ K$ whence $T_2 = 293K$ and $T_2 = 400K$ because they are $\bar{x} = 40$ and $\bar{x} = 100$ the diagrams show the concentration of.

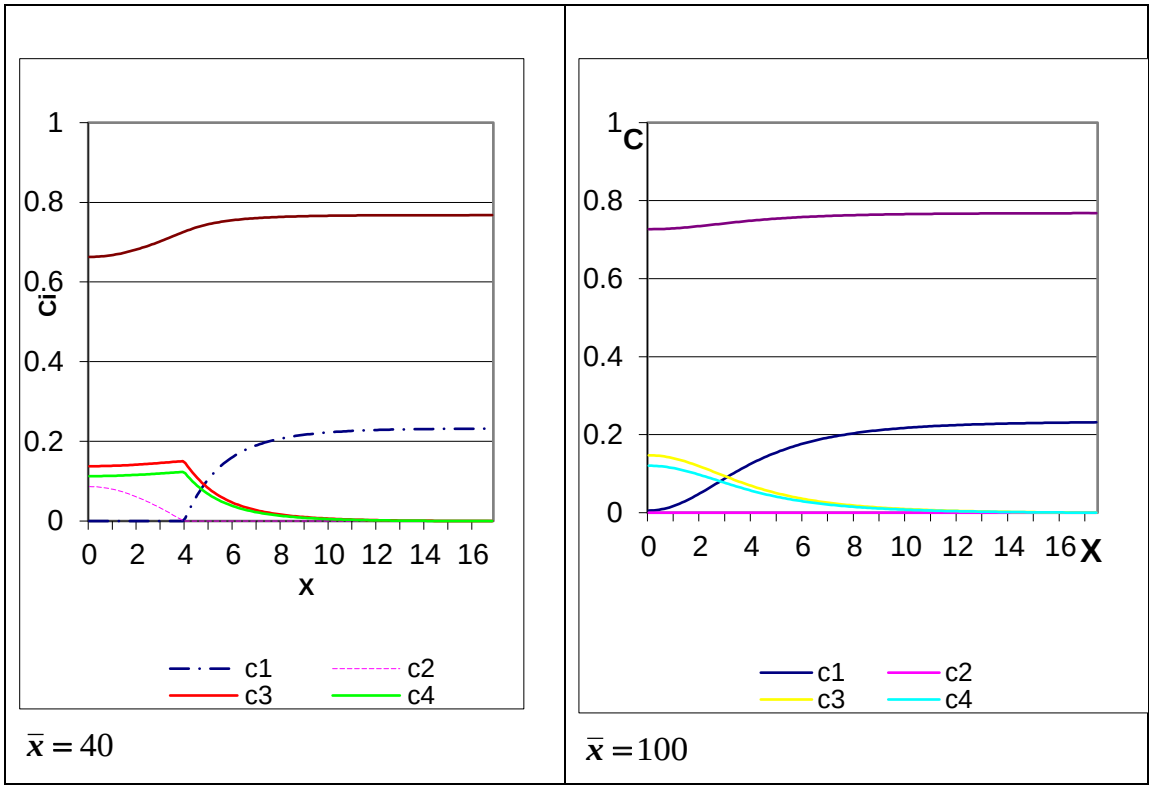

Fig. 2. $T_1 = 1000K$ and $T_2 = 293K$ of concentrations.

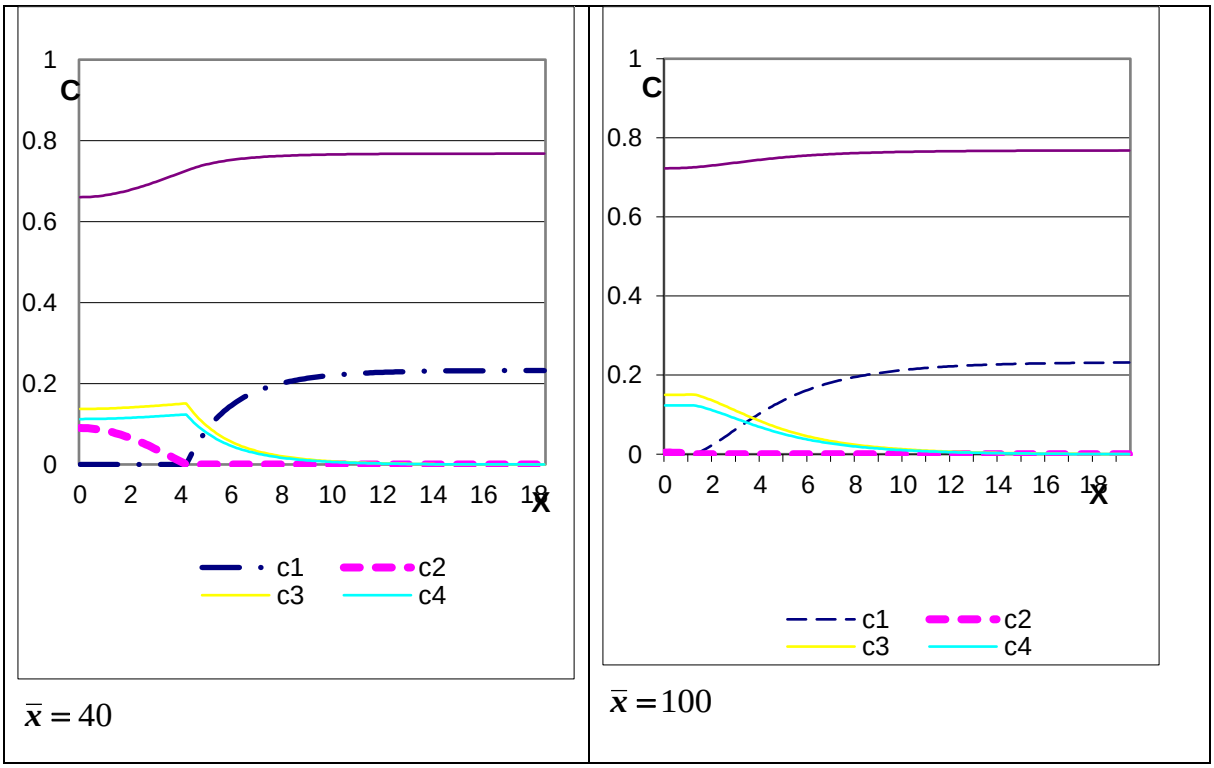

Fig. 3. $T_1 = 1000K$ and $T_2 = 400K$ of concentrations.

As you can see from this graph, $\bar{x} = 40$ the fuel core is broken.

Concentration view after the flame $T_1 = 1000K$ and $T_2 = 293K$, $\bar{x} = 100$ as shown in the diagram above. $T_1 = 1000K$ and $T_2 = 400K$ when $\bar{x} = 100$ in the cross-section. From these results we can conclude that combustion will last longer if the temperature is higher. The same results were obtained for velocity, full enthalpy, and intensity, which were much smaller than the initial flame length.

The results obtained from the same data in the introduction indicated that methane flame is short and wide, compared to propane. This can be explained by the small amount of methane flux impulse.

$T_1 = 1000\ K$ when $T_2 = 293\ K$ and $T_2 = 400K$ here is an example of the isotherms that are

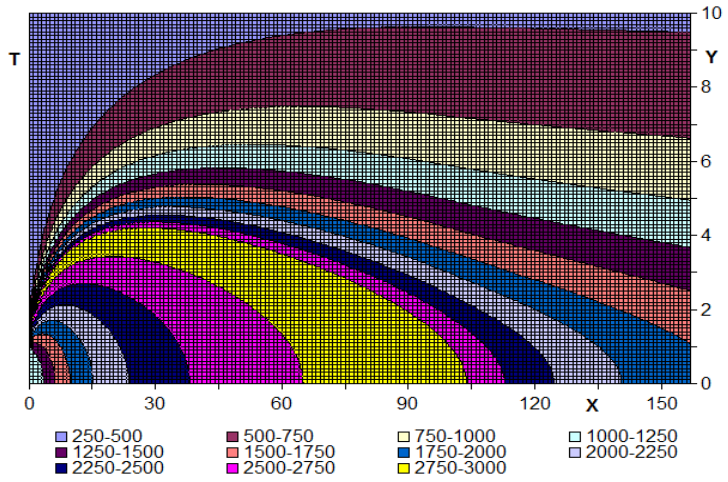

Fig. 4. $T_1 = 1000\ K$ and $T_2 = 293\ K$

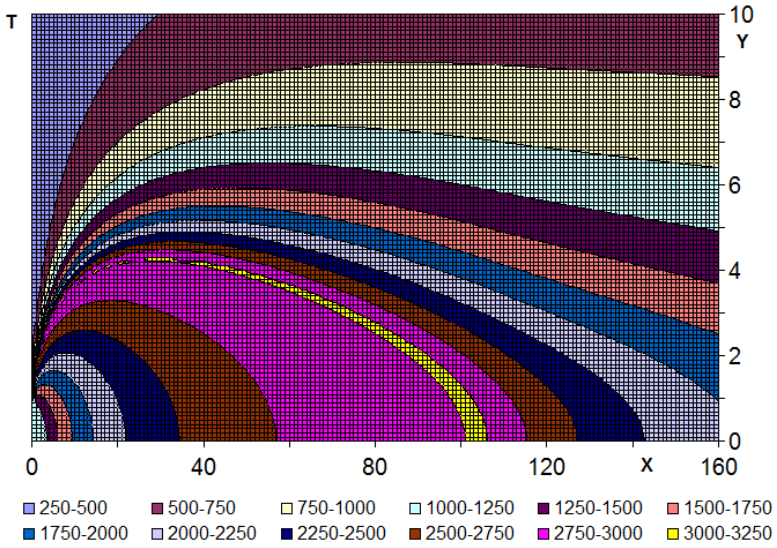

Fig. 5. $T_1 = 1000\ K$ and $T_2 = 400K$

Maximum temperature in the first case T=2929K and in the latter case $T^* = 3018.84$ values were calculated.

FINDINGS

As the temperature field expands, the maximum temperature at the end of the flame is in the axis of symmetry.Calculations show that as fuel increases with gas temperatures, the length of the flames decreases. Conversely, increased air temperature leads to an increase in the length of the flame. The first is due to the reduction in fuel gas consumption, and the second is due to the high oxygen content of oxygen in the air. In general, the results show that the temperature and gauge area of the methane fuel combustion in the airflow makes a significant difference over propane.

References

1. J. H. Park, Three-Dimensional Nonequilibrium Numerical Modeling of Arc-Anode Attachment in Direct-Current Electric Arcs, Ph.D. Thesis, University of Minnesota, 2003.

2. Gordon, S. and B. J. McBride (1994). Computer program for calculation of complex chemical equilibrium compositions and applications Part I: Analysis. Reference Publication NASA-RP-1311, NASA Glenn Research Center.
3. International Energy Agency (2009). CO2 emissions from fuel combustion 2009 edition.Technical report, International Energy Agency.
4. S. B. Pope, Ten questions Concerning the Large-Eddy Simulation of Turbulent Flows, New Journal of Physics, 2004, 6(35)
5. A. A. Iordanidis and C. M. Franck, Self-consistent Radiation-based Simulation of Electric Arcs: II. Application to Gas Circuit Breakers, J. Phys. D: Appl. Phys., 2008, 41, 135206, p 1-9.
6. Абрамович Г.Н. Теория турбулентных струй. М.: «Наука». 1984. 715 с.
7. Кузнецов В.Р., Сабельников В.А. Турбулентность и горение. М.: «Наука» 1986. 288 с.
8. Баев В.К., Головичев В.К., Третьяков П.К. Горение в сверхзвуковом потоке. Новосибирск. Наука. 1984. 304 с.
9. Алиев Ф., Жумаев З.Ш. Струйные течения реагирующих газов.Ташкент, Фан, 1987.132 с.
10. Edelman R.B. and Harsha P.T. Some observations on turbulent mixing with chemical reactions//AIAA. Aerospace Science Meeting, 15-th, New-York, 1977, Technical Paper, pp. 55-102.
11. "Numerical Grid Generation," ed. J. F. Thompson, Elsevier Sci. Pub., (1982).
12. Launder, B. E. and D. B. Spalding, "The Numerical Calculation fo Turbulent Flows, Computational Methods Applied to Mechanics and Engineering, Vol. 3,269-289, (1974).
13. Gordon, S. and B. J. McBride, "Computer Program for Calculation of Complex Chemical Equilibrium Compositions, Rocket Performance, Incident and Reflected Shocks, and Chapman-Jonquet Detonations," NASA SP-273, (1976), new version (1989).
14. Lallemant, N., R. Dugue, and R. Weber (2003). Measurements techniques for studying oxy-natural gas ames. Journal of the Institute of Energy 76.
15. Yin, C., L. C. R. Johansen, L. Rosendahl, and S. Kr (2010). Models for gas radiation properties applicable to CFD modeling of oxy-fuel combustion. Paper submitted to the 33r